

Analytical Formulae for the Surface Green's Functions of Graphene and 1T' MoS₂ Nanoribbons

Hans Kosina and Heribert Seiler
Institute for Microelectronics
 TU Wien, Vienna, Austria
 {kosina,seiler}@iue.tuwien.ac.at

Viktor Sverdlov
*Christian Doppler Laboratory for Nonvolatile Magnetoresistive
 Memory and Logic at the Institute for Microelectronics*
 TU Wien, Vienna, Austria
 sverdlov@iue.tuwien.ac.at

Abstract—Surface Green's functions describe the coupling of the device region with the attached leads. A lead represents a semi-infinite region with uniform properties such as cross section and electrostatic potential. The scattering states in the leads can be determined in different ways. In this work we exploit the uniformity of the system and formulate the problem in reciprocal space where the Green's function takes on a simple form. A Fourier transformation yields the elements of the Green's function in real space. We present the principal steps of this calculation and discuss results for nanoribbons. The 2D materials considered are graphene and MoS₂ in the 1T' phase, their electronic structure is represented by k·p Hamiltonians.

Index Terms—surface Green's functions, ballistic transport, nanoribbon, NEGF method, k·p method

I. INTRODUCTION

In the non-equilibrium Green's function formalism, open system boundary conditions are introduced by means of the retarded contact self energies. These quantities are calculated from the retarded surface Green's functions of the semi-infinite leads which are attached to the spatially finite device. There exist both iterative [1] and direct methods [2] [3] for the numerical calculation of the surface Green's function (GF). The direct method is generally more efficient than the iterative one [3].

In this work we present a k -space method for the direct evaluation of the surface GF. If the size of the matrix elements of the Hamiltonian is small, which can be the case, for instance, in 1D systems described by a k·p Hamiltonian, explicit expressions for the surface GF can be derived.

Discretization of the Hamiltonian of the semi-infinite lead yields an infinite system of difference equations.

$$\begin{aligned} (E\underline{I} - \underline{H}_{00})\underline{g}_{00} - \underline{H}_{01}\underline{g}_{10} &= \underline{I} \\ -\underline{H}_{10}\underline{g}_{n-1,0} + (E\underline{I} - \underline{H}_{00})\underline{g}_{n0} - \underline{H}_{01}\underline{g}_{n+1,0} &= 0 \\ n &\geq 1 \end{aligned} \quad (1)$$

Here, E is the energy. The underlined symbols represent matrices of order N . It holds $\underline{H}_{10} = \underline{H}_{01}^\dagger$. The element \underline{g}_{00} associated with the left surface of the lead is sought.

This work has been partly funded by the Austrian Science Fund (FWF), project P33151.

II. THEORY

In the first step we consider the infinite lead which is described by a system of difference equations of the form

$$-\underline{H}_{10}\underline{y}_{n-1} + (E\underline{I} - \underline{H}_{00})\underline{y}_n - \underline{H}_{01}\underline{y}_{n+1} = \underline{r}_n. \quad (2)$$

The index n ranges from $-\infty$ to ∞ . The right hand side is defined as $\underline{r}_n = \delta_{n,0}\underline{I}$ and represents an impulse applied at point $n = 0$. The Fourier transforms of the discrete functions \underline{y}_n and \underline{r}_n are given by the respective Fourier series.

$$\underline{Y}(k) = \sum_{n=-\infty}^{\infty} \underline{y}_n e^{inka} \quad (3)$$

$$\underline{R}(k) = \sum_{n=-\infty}^{\infty} \underline{r}_n e^{inka} = \underline{I} \quad (4)$$

Conversely, the unknowns \underline{y}_n are obtained as the Fourier coefficients of $\underline{Y}(k)$.

$$\underline{y}_n = \frac{1}{k_0} \int_0^{k_0} \underline{Y}(k) e^{-ikna} dk \quad (5)$$

Here $na = x_n$ is the coordinate of the n -th grid point and a the grid spacing. The period is $k_0 = 2\pi/a$. The Fourier transform of the equation system (2) gives a single equation in reciprocal space,

$$\underline{A}(k, E)\underline{Y}(k, E) = \underline{I}, \quad (6)$$

where

$$\begin{aligned} \underline{A}(k, E) &= \underline{A}_{-1} e^{-ika} + \underline{A}_0(E) + \underline{A}_1 e^{ika} \\ \underline{A}_{-1} &= -\underline{H}_{01}, \quad \underline{A}_0(E) = E\underline{I} - \underline{H}_{00}, \quad \underline{A}_1 = -\underline{H}_{10} \end{aligned} \quad (7)$$

Equation (6) has the formal solution

$$\underline{Y} = \underline{A}^{-1}. \quad (8)$$

Defining the characteristic polynomial $D(k, E) = \text{Det}(\underline{A})$, and designating the adjugate of \underline{A} as $\underline{B} = \text{adj}(\underline{A})$, the inverse of \underline{A} can be written as

$$\underline{Y}(k, E) = \frac{1}{D(k, E)} \underline{B}(k, E) \quad (9)$$

It holds $\underline{A}\underline{B} = D\underline{I}$. Note that \underline{A} , \underline{B} , and D are complex trigonometric polynomials: \underline{A} of degree one according to (7), D of degree N , and \underline{B} of degree $N - 1$:

$$\underline{B} = \sum_{l=1-N}^{N-1} \underline{B}_l e^{ila} \quad (10)$$

In analytical calculations the adjugate matrix can be conveniently determined using the Cayley-Hamilton theorem. From the Fourier expansion of the reciprocal of the determinant

$$\frac{1}{D(k, E)} = \sum_{n=-\infty}^{\infty} c_n e^{ink_a}, \quad c_n = \frac{1}{k_0} \int_0^{k_0} \frac{e^{-ink_a}}{D(k, E)} dk \quad (11)$$

we obtain the \underline{y}_n by a convolution of the form

$$\underline{y}_n = \sum_{l=1-N}^{N-1} c_{n-l} \underline{B}_l \quad (12)$$

Introducing the complex variable $u = \exp(ika)$ the integral in (11) turns into a contour integral over the unit circle in the complex plane. For given E , the characteristic equation $D(k, E) = 0$ has $2N$ solutions k_1, k_2, \dots, k_{2N} which always occur in pairs $\pm k_i$. Thus the poles in the integral in (11) also occur in pairs u_i and u_i^{-1} . The contour integral is evaluated by virtue of the residue theorem. The system (2) has two solutions, known as the retarded and the advanced GF, respectively. For a propagating mode in the lead the wave number k_i is real and the pole u_i is located on the unit circle. To select the retarded GF one adds a small damping term $i\eta$ to the Hamiltonian and keeps only the convergent terms. The damping term moves the poles u_i associated with a positive group velocity into the unit circle, such that their residues contribute to the integral, whereas the complementary poles u_i^{-1} move outwards and have no effect.

A. Impulse Response in the Semi-infinite Lead

The coefficients (12) represent the impulse response in the infinite domain. To describe a semi-infinite lead one has to truncate the domain by imposing the boundary condition (BC) $\underline{g}_{-1,0} = \underline{0}$. This BC can be matched by adding to the particular solution \underline{y}_n a homogeneous solution. The latter can be created by applying an impulse outside the domain of interest, that is at some negative m . Any impulse within the negative domain will emit a right traveling wave into the positive domain. This wave satisfies the homogeneous difference equations for all $n \geq 0$. The homogeneous solution is specified up to a free, constant matrix which is determined from the BC $\underline{g}_{-1,0} = \underline{0}$. This procedure yields the GF for the left surface.

$$\underline{g}_{00} = \underline{y}_0 - \underline{y}_m \underline{y}_{m-1}^{-1} \underline{y}_{-1} \quad (13)$$

The GF for the right surface can also be calculated from the impulse response \underline{y}_n . In this case the system has to be truncated at $n = 1$ by imposing the BC $\underline{g}_{10} = \underline{0}$.

III. GRAPHENE NANORIBBON

We apply the method to the Dirac-like Hamiltonian of graphene:

$$\underline{H}(k_x, k_y) = \begin{pmatrix} U_0 & \hbar v_F(k_x - ik_y) \\ \hbar v_F(k_x + ik_y) & U_0 \end{pmatrix}$$

In a nanoribbon the transverse momentum is quantized. Thus k_y can be treated as a constant parameter that represents a particular subband. Substituting $k_x = -i\partial_x$ and approximating the derivative by a central difference quotient yields a system of difference equations of the form (1) with the matrices

$$\underline{H}_{00} = ck_y \begin{pmatrix} 0 & -i \\ i & 0 \end{pmatrix}, \quad \underline{H}_{01} = \frac{c}{2ia} \begin{pmatrix} 0 & 1 \\ 1 & 0 \end{pmatrix} \quad (14)$$

Here we have set the on-site potential to $U_0 = 0$ and introduced the parameter $c = \hbar v_F$. The characteristic equation is quadratic and has two solutions. According to the residue theorem only that solution (k_0) associated with a positive group velocity has to be considered for the retarded GF. The result from our method is

$$\underline{g}_{00} = \frac{4a^2}{c^2} \frac{u_0^2}{u_0^2 - 1} (E\underline{I} + \underline{H}_{00}) \quad (15)$$

In [4] the very same expression has been obtained in a different way. Because of the simple structure of \underline{H}_{01} , the iteration series of the Sancho-Rubio method can be summed up analytically.

IV. MOS₂ NANORIBBON

Recently it has been discovered that MoS₂ in the 1T' phase is a topological insulator [5]. The inverted band structure is well described by a parabolic dispersion relation. The effective Hamiltonian is of the form [5]

$$\underline{H}(k_x, k_y) = \begin{pmatrix} \delta - c_1 k_x^2 - c_2 k_y^2 & c_6 k_y - \alpha E_z + ic_5 k_x \\ c_6 k_y - \alpha E_z - ic_5 k_x & -\delta + c_3 k_x^2 + c_4 k_y^2 \end{pmatrix}$$

with the coefficients

$$c_1 = \frac{\hbar^2}{2m_x^p}, \quad c_2 = \frac{\hbar^2}{2m_y^p}, \quad c_3 = \frac{\hbar^2}{2m_x^d}, \quad c_4 = \frac{\hbar^2}{2m_y^d} \\ c_5 = \hbar v_1, \quad c_6 = \hbar v_2$$

Here the x -axis represents the longitudinal direction, the y -axis the transverse direction, and the z -axis the direction perpendicular to the nanoribbon.

A. Bulk Dispersion Relation

The characteristic polynomial is of second degree in E .

$$p(k_x^2, k_y^2, E) = -[c_5^2 k_x^2 + (c_6 k_y - \alpha E_z)^2 \\ + (c_1 k_x^2 + c_2 k_y^2 - \delta + E)(c_3 k_x^2 + c_4 k_y^2 - \delta - E)] \quad (16)$$

Its roots $E_{1,2}(k_x, k_y)$ represent the two branches of the bulk dispersion relation. In the following we use the parameter values reported in [5]. Wavenumbers are scaled with k_0 ,

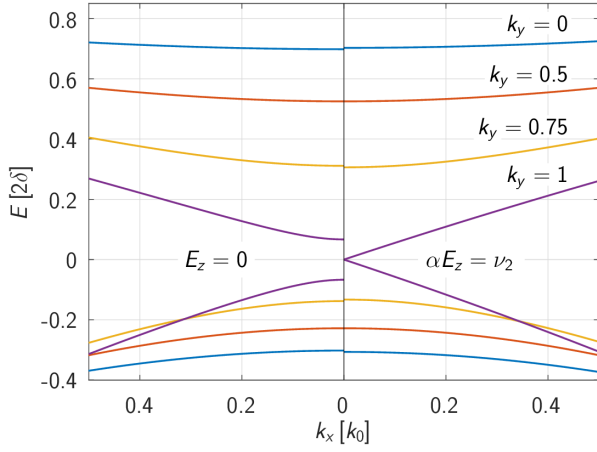


Fig. 1. Cuts of the bulk dispersion of 1T' MoS₂ at different values k_y . The bandgap at $E_z = 0$ (left panel) gets closed at $\alpha E_z = \nu_2$ (right panel).

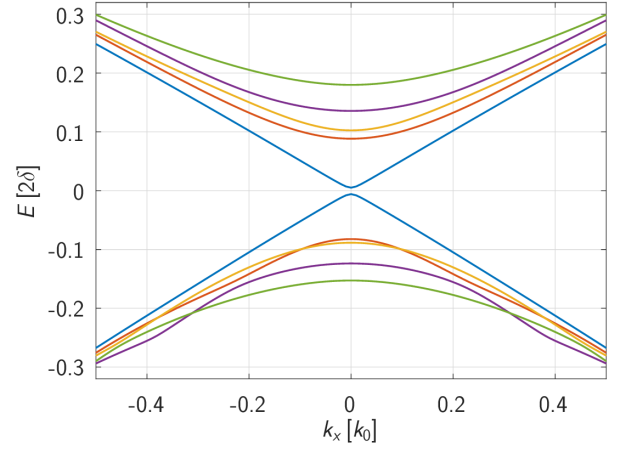


Fig. 2. Subband structure of the nanoribbon at $E_z = 0$. The subbands with a nearly linear dispersion correspond to the topologically protected edge states.

whereas energies are scaled with 2δ and offset by ΔE as suggested in [6].

$$k_0 = \sqrt{\frac{4\delta}{\hbar^2} \frac{m_y^d m_y^p}{m_y^d + m_y^p}}, \quad \Delta E = \frac{1}{2} \frac{m_y^d - m_y^p}{m_y^d + m_y^p} \quad (17)$$

In Fig. 1 cuts of the bulk dispersion at different values of k_y are shown. The bandgap at $(k_x, k_y) = (0, 1)$ which is finite at $E_z = 0$ (left panel) closes at $\alpha E_z = \nu_2$ (right panel) and reopens when E_z is further increased [6].

B. The Subband Structure

The characteristic polynomial (16) is of fourth degree in k_y . The roots are designated as k_y^j with $j = 1, 2, 3, 4$. We choose a mode space approach and express the transverse modes as linear combinations of the four basis functions $\exp(ik_y^j y)$. The two spinor components have to satisfy homogeneous Dirichlet BCs at the two edges of the nanoribbon. These BCs yield a system of four homogeneous equations with a coefficient matrix \underline{M} [6]. The Schrödinger equation and the characteristic equation for the BCs,

$$\begin{aligned} \text{Det}(\underline{E}\underline{I} - \underline{H}) &= 0, \\ \text{Det}(\underline{M}) &= 0, \end{aligned}$$

are solved simultaneously using the Newton method. In this way the discrete eigen-energies E and the related transverse momenta k_y^j for a given k_x can be computed.

We assume a nanoribbon width of $d = 40/k_0 = 28.86$ nm. Five electron and hole subbands at $E_z = 0$ are depicted in Fig. 2. The dispersions of the lowest electron and topmost hole subbands are linear. The energies of these subbands lie in the bulk bandgap (Fig. 1, left panel). These subbands correspond to the topologically protected edge states as the related wave functions are localized at the edges.

Fig. 3 shows the subband structure at an electric field of $\alpha E_z = \nu_2$. While the bandgap of the bulk material would

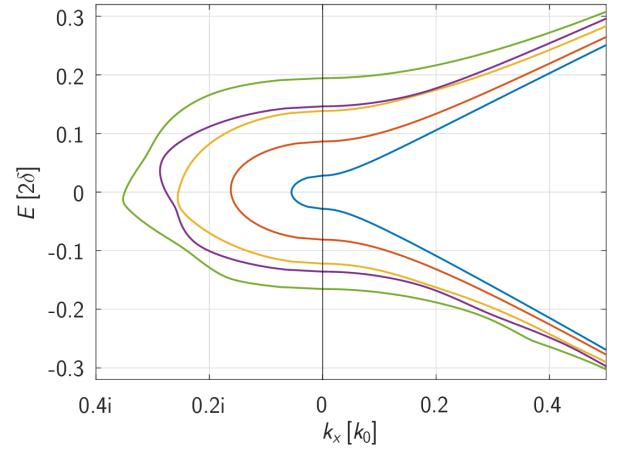


Fig. 3. Complex subband structure of the nanoribbon at $\alpha E_z = \nu_2$.

be closed at this field strength, it remains finite in a narrow nanoribbon. Transistor action can be achieved by applying a vertical field over a finite region of the nanoribbon, which represents the channel region. In the off-state, electrons in the leads ($E_z = 0$) would be blocked by the finite bandgap in the channel. In this situation tunneling through the gap has to be considered, which require knowledge of the complex band structure (Fig. 3, left panel).

C. Contact Self Energy

After the substitution $k_x = -i\partial_x$ and applying the central difference approximation the Hamiltonian of the nanoribbon becomes a block-tridiagonal matrix with the following 4×4 blocks.

$$\underline{H}_{00} = \begin{pmatrix} \underline{T} & \underline{S} \\ \underline{S}^\dagger & \underline{T} \end{pmatrix}, \quad \underline{H}_{01} = \begin{pmatrix} \underline{R} & \underline{0} \\ \underline{S} & \underline{R} \end{pmatrix} \quad (18)$$

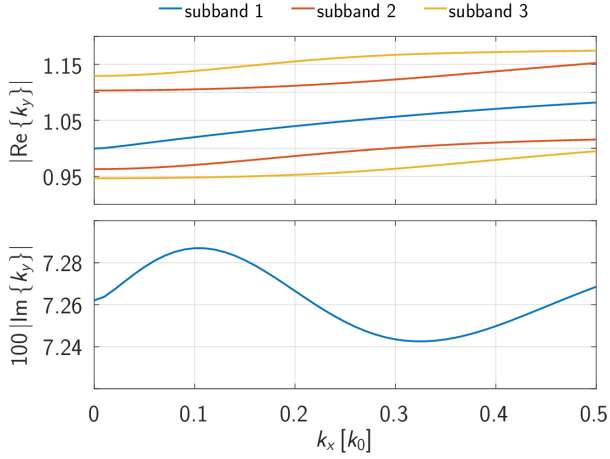


Fig. 4. Absolute values of $\text{Re}\{k_y\}$ and $\text{Im}\{k_y\}$ as functions of the longitudinal wave number k_x . Only the lowest subband develops an imaginary part which causes the formation of edge states. The higher subbands have real wave numbers which describe simple standing waves in the transverse direction.

Here,

$$\underline{R} = \frac{1}{4a^2} \begin{pmatrix} c_1 & 0 \\ 0 & -c_3 \end{pmatrix}, \quad \underline{S} = \frac{c_5}{2a} \begin{pmatrix} 0 & 1 \\ -1 & 0 \end{pmatrix} \quad (19)$$

and $\underline{T} = \underline{H}(0, k_y) - 2\underline{R}$.

To describe the discrete system one has to replace k_x with \tilde{k}_x defined as

$$\tilde{k}_x = k_x \text{sinc}(k_x a) \quad (20)$$

We introduce the complex variable $u = e^{2ik_x a}$ and express \tilde{k}_x^2 as $\tilde{k}_x^2 = (2 - u - u^{-1})/(4a^2)$. The characteristic polynomial of the discrete system is related to (16) by the following transformation.

$$f(u, k_y, E) = u^2 p((2 - u - u^{-1})/(4a^2), k_y, E) \quad (21)$$

The characteristic equation $f(u) = 0$ has to be solved for a given energy E and a wavenumber k_y characteristic of a given subband. The transverse wavenumbers k_y depend weakly on the longitudinal wavenumber k_x as shown in Fig. 4. To enable one-dimensional transport calculations in mode space one has to neglect this dependence and assume a constant k_y . For energies close to the subband minimum one can use the approximation $k_y(k_x) \approx k_y(0)$.

For an energy E_0 inside a given subband (outside the bandgap) the equation $p(k_x^2, k_y, E_0) = 0$, or equivalently the equation $E(k_x, k_y) = E_0$, has two real solutions $\pm k_x^{(1)}$. Due to the monotonicity of the dispersion relation, see Fig. 2, there can exist only two real solutions, and thus the remaining two solutions $\pm k_x^{(2)}$ must be complex.

The roots $u_{1,3} = \exp(\pm 2ik_x^{(1)} a)$ are located on the unit circle. The root associated with positive group velocity we designate as u_1 . One of the two complex solutions $\pm k_x^{(2)}$ gives a root u_2 inside the unit circle, whereas the complementary root $u_4 = u_2^{-1}$ is located outside.

Having identified the roots relevant to the retarded GF we can now apply the residue theorem to determine the coefficients (11).

$$c_n = \frac{u_1^{1+|n|}}{f'(u_1)} + \frac{u_2^{1+|n|}}{f'(u_2)} \quad (22)$$

Following the procedure outlined in Section II we arrive at the surface GF. We summarize the result for contact self energy which is defined as $\underline{\Sigma} = \underline{H}_{01} \underline{g}_{00} \underline{H}_{10}$. First, one has to set up four matrices:

$$\begin{aligned} \underline{U} &= \underline{H}_{01} [(E - \text{Tr}(\underline{T})) \underline{I} + \underline{H}_{00}] \underline{H}_{10} \\ \underline{\sigma}_1 &= \mu_1 \underline{U} + D(\mu_2 \underline{H}_{01} + \underline{H}_{10}) \\ \underline{\sigma}_2 &= \underline{U} + \mu_1 D(\underline{H}_{01} + \underline{H}_{10}) \\ \underline{\sigma}_3 &= \mu_1 \underline{U} + D(\underline{H}_{01} + \mu_2 \underline{H}_{10}) \end{aligned}$$

where $\mu_1 = c_1/c_0$, $\mu_2 = c_2/c_0$, and $D = -\text{Det}(\underline{R})$. Then the contact self energy is obtained as

$$\underline{\Sigma} = c_0 [\underline{\sigma}_2 - \underline{\sigma}_3 \underline{\sigma}_2^{-1} \underline{\sigma}_1] \quad (23)$$

The results of this derivation have been verified numerically. The computed surface GF satisfies the quadratic matrix equation

$$(\underline{E}\underline{I} - \underline{H}_{00} - \underline{H}_{01} \underline{g}_{00} \underline{H}_{10}) \underline{g}_{00} = \underline{I}, \quad (24)$$

whereas the computed matrices \underline{y}_n satisfy the difference equations (2).

REFERENCES

- [1] M. P. L. Sancho, J. M. L. Sancho, J. M. L. Sancho, and J. Rubio, "Highly convergent schemes for the calculation of bulk and surface green functions," *Journal of Physics F: Metal Physics*, vol. 15, no. 4, pp. 851–858, apr 1985.
- [2] R. C. Bowen, W. R. Frenseley, G. Klimeck, and R. K. Lake, "Transmission resonances and zeros in multiband models," *Phys. Rev. B*, vol. 52, pp. 2754–2765, Jul 1995.
- [3] M. Luisier, A. Schenk, W. Fichtner, and G. Klimeck, "Atomistic simulation of nanowires in the $sp^3 d^5 s^*$ tight-binding formalism: From boundary conditions to strain calculations," *Phys. Rev. B*, vol. 74, p. 205323, Nov 2006.
- [4] S.-K. Chin, K.-T. Lam, D. Seah, and G. Liang, "Quantum transport simulations of graphene nanoribbon devices using Dirac equation calibrated with tight-binding π -bond model," *Nanoscale Research Letters*, vol. 7, no. 1, p. 114, 2012.
- [5] X. Qian, J. Liu, L. Fu, and J. Li, "Quantum spin Hall effect in two-dimensional transition metal dichalcogenides," *Science*, vol. 346, no. 6215, pp. 1344–1347, 2014.
- [6] V. Sverdlov, A.-M. B. El-Sayed, H. Kosina, and S. Selberherr, "Conductance in a nanoribbon of topologically insulating MoS₂ in the 1T phase," *IEEE Transactions on Electron Devices*, 2020 (submitted).